# Influence of Thermomechanical Processing on Low Cycle Fatigue of Prealloyed Ti-6Al-4V Powder Compacts

D. EYLON, F. H. FROES, D. G. HEGGIE, P. A. BLENKINSOP, and R. W. GARDINER

A wide range of microstructures was generated using various thermomechanical processing sequences in Ti-6Al-4V Rotating Electrode Process (REP) powder compacts of low contaminant content. Low cycle fatigue results were found to be superior to those in higher contaminant compacts tested in a previous program. All microstructural groups showed fatigue strengths equivalent to those found in wrought alloy, with the beta-annealed condition being lowest as expected. Alpha + beta work and solution treatment resulted in an excellent fatigue strength of 875 $MN/m^2$ (127 ksi) at $10^5$ cycles; 85 pct of the UTS. In the five conditions tested, the fatigue strength increased with increasing tensile strength, decreasing grain size, and increasing volume fraction of low aspect ratio primary alpha. Most crack initiation sites were observed at the specimen surface. Only alpha + beta worked and solution-treated material exhibited subsurface initiations, none of which was associated with any defect or with a lower fatigue life. Although compacts contained some tungsten particles, in no case were they associated with crack initiation sites, indicating that they were innocuous in the conditions evaluated.

## I. INTRODUCTION

RECENT developments in titanium powder metallurgy (PM) have been aimed at producing lower cost components, while maintaining mechanical properties at least equivalent to those exhibited by wrought material.[1–4] The static properties of PM Ti-6Al-4V, such as tensile behavior and fracture toughness, have been found to be equal to wrought levels. However, dynamic properties of PM material, such as low cycle fatigue (LCF)[5] and high cycle fatigue (HCF),[6–10] in which initiation plays a major role, can be degraded as a result of high contaminant levels. These contaminants result from insufficient attention being given to cleanliness during powder production and subsequent handling. During the past decade, only one type of prealloyed powder has been available in commercial quantities: the Rotating Electrode Process (REP) powder.[11] This powder can contain various types of contaminants including: (a) tungsten particles from the tungsten cathode, (b) cross contaminant particles such as iron and superalloy powders, and (c) nonmetallic inclusions introduced during powder handling. Previous work on the effect of thermomechanical processing (TMP) on the microstructure of REP compacts indicated that mechanical behavior, LCF in particular, was degraded compared to wrought material.[5] In contrast to the majority of other results reported,[1] that work[5] also showed fatigue crack initiation predominantly at tungsten particles rather than at cross-contaminant metal particles or nonmetallic inclusions.

In the past few years, greatly improved REP powder has become available, and more recently a tungsten-free powder has been produced using a plasma source rather than the previously used tungsten arc. This new Plasma REP powder is termed PREP.[11] However, even in extremely clean powder, a few, albeit small, contaminant particles exist. Complete removal of these by cleaning would make the powder prohibitively expensive.[1,3] Thus, to make use of powder compacts in fracture critical applications, it is necessary either to accept some degradation in defect sensitive mechanical property behavior or to render innocuous the foreign particles present. One way to achieve this latter objective is to reduce the content of the contaminants below some critical levels. The levels required have been defined for superalloys,[12] and a parallel study to determine these levels in the titanium system[13] is currently in progress. The critical parameters are likely to vary with changes in alloy strength level, ductility, and microstructure. It was the primary aim of the present work to vary the Ti-6Al-4V microstructure by TMP, and to investigate whether this would make consolidated powder less sensitive to premature crack initiation at tungsten or other contaminant particles in LCF tests. The REP powder used in this work was the cleanest available at the time the program was initiated and was produced using practices designed to give low tungsten and low cross-contaminant/nonmetallic inclusion contents. This powder was therefore used for the program knowing that when PREP powder became available, it would be even cleaner as no tungsten would be present and a facility dedicated to titanium would be used.[11] Since tungsten particles had been the predominant LCF initiation sites in the earlier work, it was felt that the cleaner REP compacts should exhibit superior mechanical properties.

## II. EXPERIMENTAL PROCEDURES AND RESULTS

### A. *Material*

Two Ti-6Al-4V REP powder compacts were HIP consolidated by Colt Industries, Crucible Compaction Metals Operation at 915 °C (1685 °F) for six hours at 1 Kbar (15 ksi) pressure using the ceramic mold process.[14] The compacted logs measured 95 mm (3.75 inches) diameter by

D. EYLON, Principal Investigator, Metcut-Materials Research Group, P.O. Box 33511, and F. H. FROES, Technical Area Manager, Air Force Wright Aeronautical Laboratories, Materials Laboratory, Structural Metals Branch, are at Wright-Patterson AFB, OH 45433. D. G. HEGGIE and P. A. BLENKINSOP are with IMI Titanium, IMI Kynoch Ltd., Research and Development Department, Witton, Birmingham, B6 7BA, United Kingdom. R. W. GARDINER is with Royal Aircraft Establishment, Materials Department, Farnborough, Hampshire, GU14 6TD, United Kingdom.
Manuscript submitted September 9, 1982.

Table I. Chemical Compositions — Wt Pct

| Element | Al | V | Fe | C | $N_2$ | $O_2$ | $H_2$ | W | Ti |
|---|---|---|---|---|---|---|---|---|---|
| Present work | 6.1 | 4.1 | 0.21 | 0.01 | 0.026 | 0.198 | 0.0177 | 0.004 | Bal. |
| Previous work | 5.8 | 4.4 | 0.08 | N/A | N/A | 0.116 | N/A | 0.024 | Bal. |

Table II. Thermomechanical Processing Conditions

| Condition Number | Final Forging Temperature °C (°F) | Heat Treatment °C (°F) | Annealing Treatment °C (°F) | Condition Designation |
|---|---|---|---|---|
| 1 | — | — | — | as-HIP'd |
| 2 | — | 960 (1760)/1h/WQ | 700 (1290)/2h/AC | HIP'd + H. T. |
| 3 | 950 (1740) | 920 (1685)/4h/FC | — | HIP'd + hot work + HIP thermal cycle |
| 4 | 950 (1740) | 960 (1760)/1h/WQ | 700 (1290) /2h/AC | HIP'd + hot work + H. T. |
| 5 | — | 1040 (1900)/1h/FC | 730 (1350)/4h/AC | HIP'd + beta annealed |

200 mm (8 inches) long and weighed approximately 5 kg (10.5 pounds) each. The chemical analysis of the compacts is listed in Table I and is compared to the chemistry of material used in the previous work.[5] The most significant differences in chemistry are in oxygen and tungsten contents.

### B. *Thermomechanical Processing*

Five microstructural conditions were developed by thermomechanical processing as listed in Table II. The forging of Conditions 3 and 4 material was performed on a 500 metric ton hydraulic Lombard press, operated in a constant crosshead speed mode. An adjustable width channel resistance heated hot die set-up was used, which confined the forging width and allowed the workpiece to elongate. A three-step forging process was used with two steps at 1125 °C (2060 °F) and final forge at 950 °C (1740 °F). Based on cross-section area reduction, the total deformation was 56 pct with most of the work being done at the lower temperature. In all three steps, the dies were heated to 950 °C (1740 °F) and a 0.5 hour soak-time was used.

### C. *Microstructural Conditions*

Photomicrographs of all five conditions are shown in Figures 1(a) through 1(e).

*Condition 1* is the baseline as-HIP'd microstructure consisting of a low aspect ratio alpha plate structure.

*Condition 2* has a microstructure developed using a near-transus alpha + beta solution treatment. It combines about 50 vol pct primary alpha remnant of the as-HIP'd structure, which is crack initiation resistant in low[15] and high[16] cycle fatigue, in a matrix of highly crack propagation resistant, fine transformed beta structure.[17]

*Condition 3* simulates the HIP thermal cycle (same temperature, time, and cooling rate) in an alpha + beta worked material. This condition thus allows a direct determination of the effect of hot-work alone on the fatigue by comparing Conditions 1 and 3.

*Condition 4* is similar to Condition 2 but the alpha + beta work produces globulization of the primary alpha (about 50 vol pct) during heat treatment.[18] The lower aspect ratio of the primary alpha was expected to improve the crack initiation resistance.[15] A similar condition was also used in the previous work.[5]

*Condition 5* is a beta annealed condition with large beta grains and colonies of high aspect ratio alpha plates. This microstructure is known to be very sensitive to defect induced crack initiation[19,20] and thus was expected to accentuate the effect of contaminants on fatigue life and show inclusions in the crack initiation sites.

Of the five microstructures tested, Condition 4 had the finest primary alpha followed by Condition 2 and Condition 3. The as-HIP'd Condition 1 displayed coarser primary alpha while the beta annealed Condition 5 could be considered as the coarsest alpha structure in this work.

### D. *Mechanical Properties*

Tensile tests were conducted both at AFWAL (USA) and IMI (UK) using specimens measuring 4 mm diameter × 16 mm long (0.16 × 0.63 inch) and 5.66 mm diameter × 28 mm long (0.22 × 1.1 inches) nominal gage lengths cut in the longitudinal direction, respectively, at approximate strain rates of 0.005 mm/mm/min (AFWAL) and 0.0025 mm/mm/min (IMI) through the 0.2 pct yield point. The test results were in very good agreement and have thus been combined in Table III; each value represents the average of at least four tests.

Only six small size fatigue specimens of each condition were tested due to the limited compacted material available. The specimen design is shown in Figure 2. Tests were conducted on a modified rupture load frame equipped with a rotating arm which loaded and unloaded weights at 0.15 Hz frequency and $R$ value (minimum stress/maximum stress) of zero.

The fatigue data points and the best fit fatigue curves for all five conditions are shown in Figure 3. These curves are compared in Figure 4 to the scatterband of the fatigue results of lower contaminant level REP powder compacts (22 ppm rather than the 40 ppm tungsten in the present work) HIP consolidated to a different microstructure and strength level of 985 MPa (143 ksi).[9,10] It should also be noted that the lower contaminant REP compact was fatigue tested at a higher frequency (5 Hz and $R = 0.1$). However, a number of Condition 1 specimens were tested under the same higher frequency fatigue conditions[21] and produced almost identical results to those of Condition 1 in the present work so these results are compatible for comparison purposes. Figure 4 also includes the fatigue data from the earlier work[5]

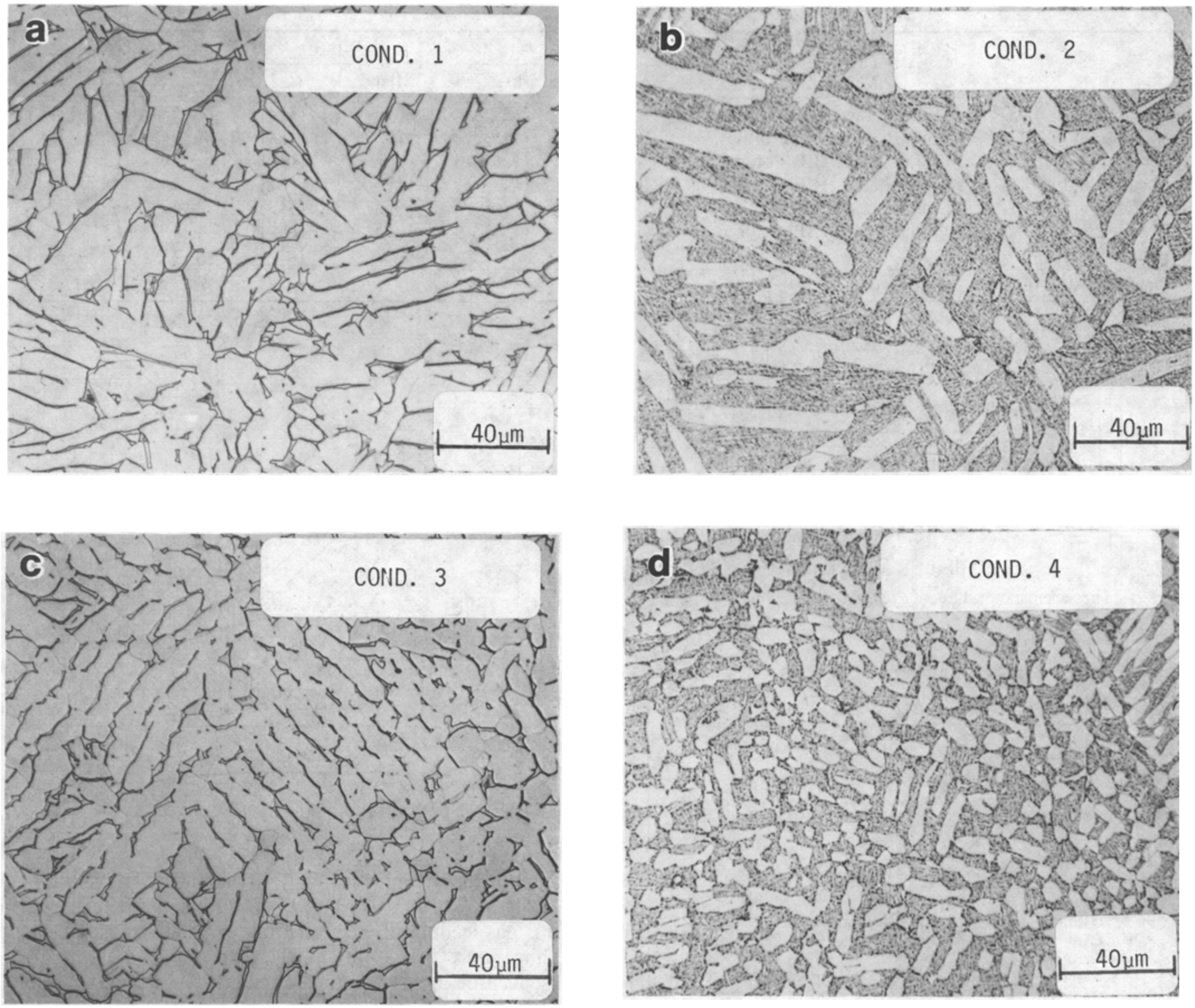


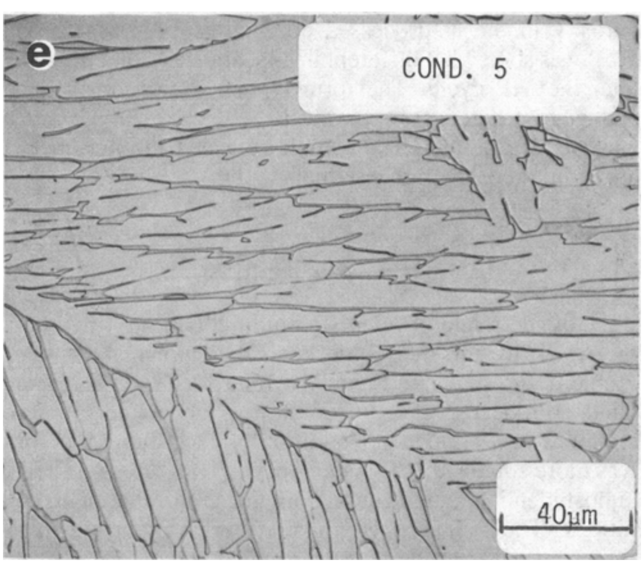


Fig. 1 — The 5 microstructures of the conditions listed in Table II. (*a*) As-HIP'd; (*b*) 960 °C solution treated + aged; (*c*) 950 °C forged + 920 °C heat treated; (*d*) 950 °C forged + 960 °C solution treated + aged; and (*e*) 1040 °C beta annealed + aged.

with microstructures equivalent to Condition 4 in the present work but with higher levels of contaminants (Table I).

### E. *Metallography and Fractography*

The origins of fatigue failure of all specimens were examined by scanning electron microscopy. Subsurface crack origins are noted by an "I" next to the individual data points, both in Figures 3 and 4. Only 5 out of the 33 tested specimens had a subsurface origin, 4 from Condition 4 group and 1 from Condition 5. No pores or inclusions were observed at those subsurface initiation sites although the compacts contained a few small pores (Figures 5(a) and 5(b)) and both metallic (including tungsten) and nonmetallic contaminants

**Table III. Tensile Test Results of Ti-6Al-4V Compacts[a]**

| | Material | 0.2 Pct Y.S. MPa | (ksi) | U.T.S. MPa | (ksi) | Elong. Pct | RA Pct |
|---|---|---|---|---|---|---|---|
| Condition 1 | 95 mm diameter, HIP billet | 875 | (127) | 995 | (144) | 16 | 37 |
| Condition 2 | 95 mm diameter, HIP billet | 1000 | (145) | 1105 | (154) | 14 | 35 |
| Condition 3 | 56 mm square, HIP + forge | 885 | (128) | 1005 | (146) | 16 | 39 |
| Condition 4 | 56 mm square, HIP + forge | 1015 | (147) | 1120 | (163) | 14 | 42 |
| Condition 5 | 95 mm diameter, HIP billet | 870 | (126) | 985 | (143) | 12 | 23 |
| Condition 4 (Previous work[5]) | 50 mm square, HIP + forge | 905 | (131) | 1025 | (149) | 19 | 40 |

[a]Combined AFWAL and IMI data

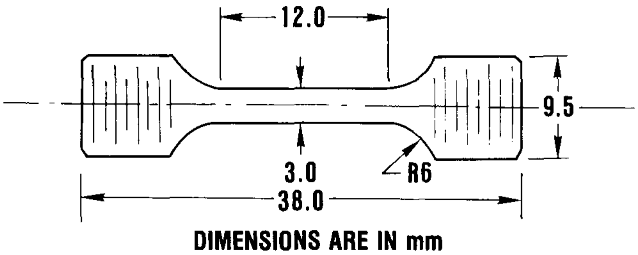

Fig. 2—The schematic of the low cycle fatigue specimen.

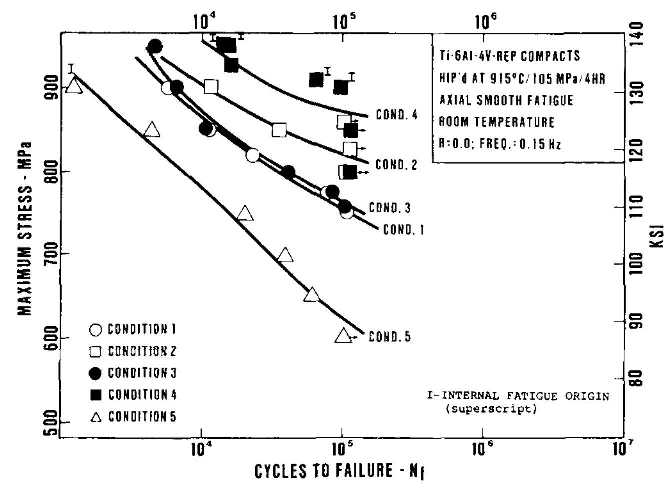

Fig. 3—Maximum stress *vs* cycles to failure S-N curves and data points of the 5 microstructural conditions.

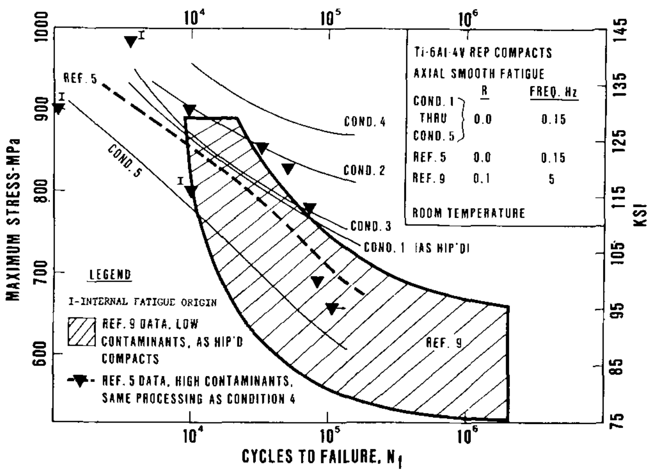

Fig. 4—The S-N curves of the present work conditions are compared to previous works data (Refs. 5 and 9).

(Figures 5(c) and 5(d)). Typical surface and subsurface initiation sites are shown in Figures 6(a), 6(b), 6(c), and 6(d), respectively.

A few small pores, of the order of a few microns in diameter, were detected both on the fracture surface near some initiation sites (Figure 7(a)) and on metallographically prepared sections for Conditions 2 through 5 (Figures 5(a) and 5(b)). Those pores were not associated with lower fatigue life, and it was concluded that their small size did not affect the crack initiation process.[13]

A thermally-induced porosity (TIP) test was conducted on a 12 mm (0.5 inch) cubic specimen of Condition 1. The specimen was vacuum heat-treated at 1300 °C (2370 °F) for two hours and slow-cooled,[22] which produced a TIP porosity of 1 vol pct (Figure 7(b)). This suggests that some argon leaked into the evacuated can during the HIP cycle resulting in as-compacted material containing argon in solution. The subsequent thermomechanical treatments of Conditions 2 through 5 or the TIP thermal cycle enhanced diffusion of this gas leading to the formation of small voids. The high temperature of the TIP test, compared to the heat treatments used in this program, resulted in an increased volume fraction of voids. However, the question of TIP porosity requires further work, since it should be noted that the porosity in the as-processed conditions (Figures 5(a) and 5(b)) was somewhat different in appearance to that produced after the TIP cycle. The former pores were not spherical and were located at prior particle boundaries. Chemical analysis of one as-HIP'd sample revealed the presence of argon but at a level of less than 1 ppm.

## III. DISCUSSION

The wide range of microstructural conditions attained in this work by the thermomechanical treatments employed (Table II) are shown in Figures 1(a) through 1(e). The simulated HIP heat cycle of Condition 3 generated a microstructure very similar to Condition 1, except that the alpha was more equiaxed.[18] The similarity of structures resulted in almost identical fatigue curves (Figure 3) for these two conditions. The fatigue strength of material evaluated in the present work exceeds that determined in an earlier evaluation of consolidated REP powder which contained a higher level of tungsten contamination[5] (Table I). The processing

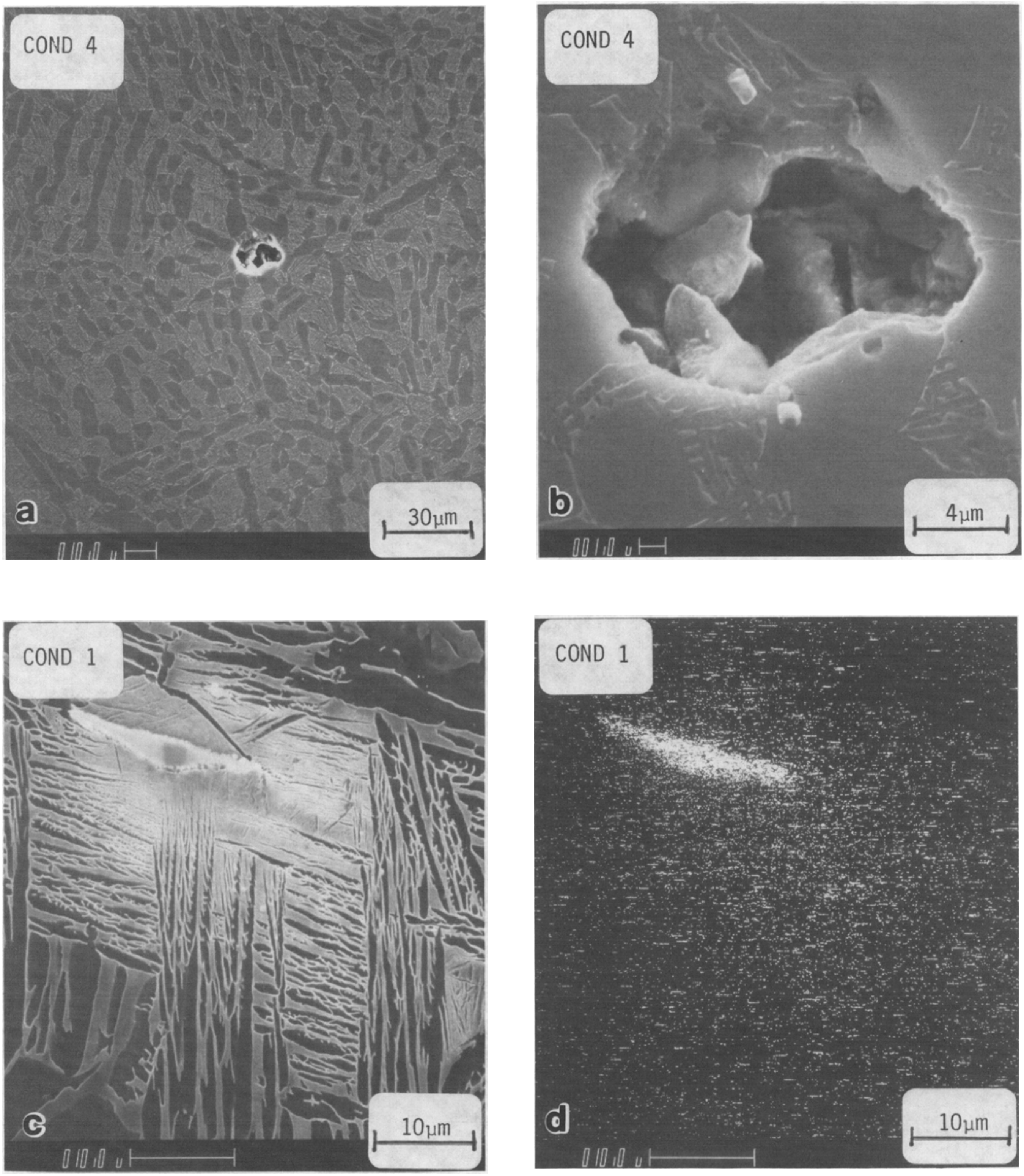


Fig. 5—(*a*) and (*b*) Low and high magnification of a micropore in Condition 4 material; (*c*) and (*d*) SEM image and X-ray image of tungsten contaminants in Condition 1 material.

parameters and microstructure of the material used in the earlier work were similar to Condition 4 in the present work (Table II). Therefore, the reduction in fatigue strength due to the high tungsten level can be shown by comparing these data to the curve for Condition 4 (Figure 4). However, it is likely that part of the fatigue degradation is due to the lower tensile strength of the material tested in the prior work (Table III). The fatigue curve for the high tungsten material (Figure 4) is clearly lower than those for all conditions in the present work except, as anticipated, for the beta annealed Condition 5. The data scatter of the high contaminant material (Figure 4) is also much larger than that for the low

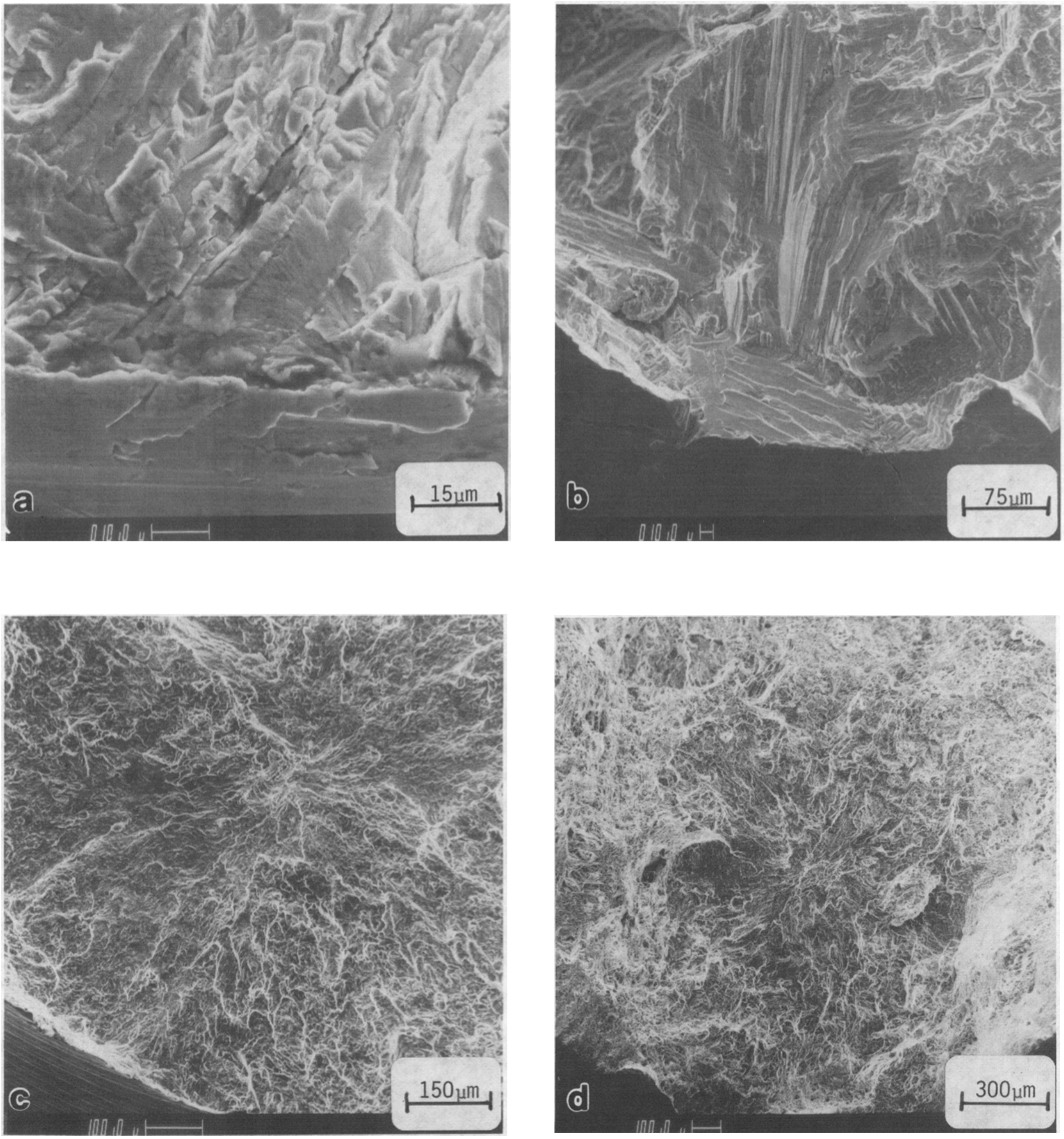


Fig. 6—(*a*) and (*b*) Faceted fatigue surface initiation in Condition 1 and 5 specimens, respectively; (*c*) and (*d*), defect-free subsurface fatigue initiations in Condition 4 specimens.

contaminant material studied in the present work (Figure 3). In the earlier work, tungsten particles were identified at internal fatigue origins and, therefore, could have contributed to a reduction in fatigue strength. In the present material, some internal origins were observed but no tungsten or other extraneous element was identified at the origin, and although some porosity was observed in the billets (Figures 5(a) and 5(b)), none appeared to be present at the origins. It must be concluded, therefore, that some of the improvements in fatigue strength, compared with earlier REP compacted material, resulted from a reduction in tungsten contamination. Some of the improvement in fatigue strength also results from the higher strength of the present material (due in part to higher levels of oxygen and iron). A cleaner PREP powder than the one used in the present work is now commercially available,[11] and based on the present data, it is reasonable to assume that the good fatigue properties will be at least maintained with the cleaner powder.

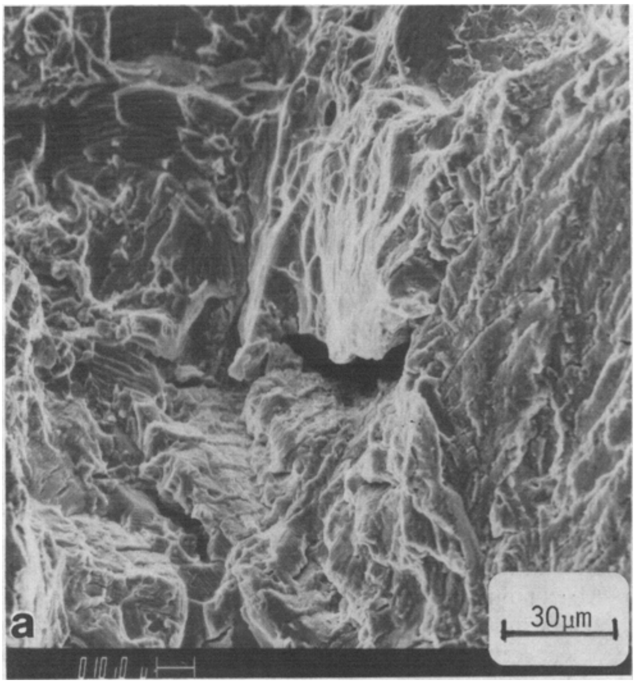


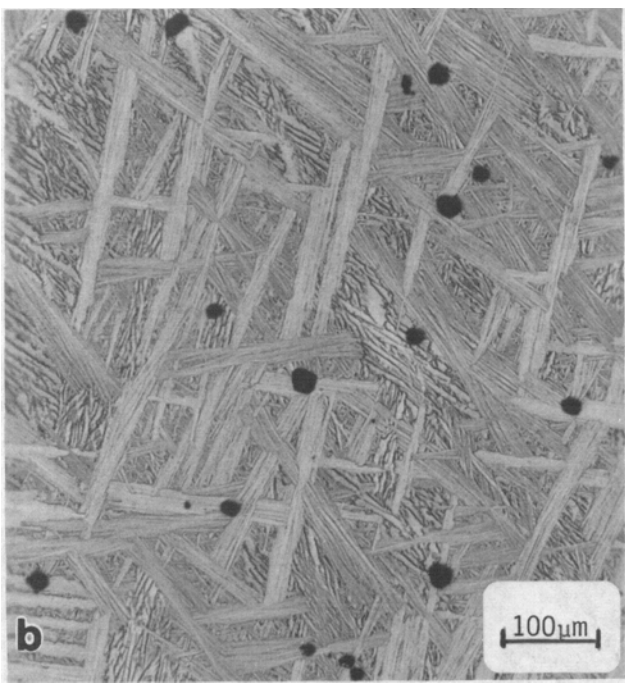


Fig. 7—(*a*) Micropore on a fatigue fracture surface (not an initiation site); (*b*) Thermally-Induced Porosity (TIP) after 1300 °C/2h thermal exposure and slow-cool in Condition 1 material.

However, it may also be necessary to improve the control of chemical composition, in particular oxygen content, if a high fatigue strength is required.

In the cases of Conditions 2 and 4, the heat treatment and/or the thermomechanical processing resulted in higher tensile strength than the other conditions. The higher fatigue strength of these conditions is probably, in part, a reflection of this strength increase. The microstructures of Conditions 2 and 4 contain about 50 vol pct of low aspect ratio primary alpha in a matrix of finely transformed beta. The lower primary alpha aspect ratio of Condition 4, its smaller size as well as the slightly higher strength level, are considered to be the cause for the better fatigue strength. This is consistent with the findings of other work where fatigue crack initiation appeared to be associated with the elongated primary alpha[9] resulting from a less extended HIP cycle (lower temperature, shorter time) than in the present work. Condition 4 produces a remarkably high fatigue strength at $10^5$ cycles of approximately 875 MN/$m^2$ (127 ksi) which is 0.85 of the UTS. The large number of subsurface initiations in this condition (four out of five failed specimens) is not understood, but is definitely not associated with lower fatigue life. All subsurface initiation sites (Figures 6(c) and 6(d)) were found to be unrelated to defects or irregularities of any sort in the microstructure. Previous work on fatigue crack initiation of wrought titanium alloys[23,24] showed that subsurface initiation could be associated with better fatigue life provided that it did not originate at material defects (pores or inclusions). A typical surface initiation location of Condition 1 specimen (Figure 6(a)) shows a faceted fracture with few alpha plates visible on this surface. This suggests that there may be some orientation relationships between adjacent alpha plates (Figure 1(a)), leading to a localized fracture mode similar to that in a beta annealed material.[25,26]

As anticipated, Condition 5 demonstrated lower fatigue life from a beta annealed microstructure.[19,20] This behavior is related to the very large crack initiation facets evident in Figure 6(b). These facets are the result of the large colonies (Figure 1(e)) of similarly aligned and crystallographically oriented alpha plates.[27] There is also evidence of secondary cracking at these locations which is typical of a large colony beta annealed structure.[19] However, it was also expected that this structure would initiate cracks at contaminants or pores[19] (which was the reason for the inclusion of this condition), but five out of six Condition 5 specimens exhibited failures starting at surface locations with no apparent relation to defects. Another typical characteristic of this coarse colony structure is fracture facets with two or more alpha plate orientations both in crack initiation (Figure 8(a)) and propagation (Figure 8(b)) locations. This was previously observed in beta annealed wrought alloys in which facets were found to be on or near $(0001)_\alpha$ planes.[25,26] This multi-colony fracture makes the potential initial crack size even larger than a colony size. In some extreme cases, the initial crack could be as large as the whole beta grain when the alpha plate colonies within a single beta grain, which relate to each other through the Burger's relationship,[25] will share common basal plane.

The additional comparison data (shaded area in Figure 4) was developed from REP low contaminant compacts in a parallel program.[9] The data from the present work (Conditions 1 through 4) show better fatigue lives at the $10^5$ cycles range even for the as-HIP'd Condition 1. This is attributed to the lower aspect ratio primary alpha plates, which result from a longer HIP time and slower cooling rate.[18] These fatigue data (a) are also at a similar level to the best results from wrought mill anneal Ti-6Al-4V material.[2]

It is important to note that the small pores observed metallographically in Conditions 2 through 5, which may be attributable to TIP, were not detrimental to fatigue life. It appears that porosity which is smaller than some critical

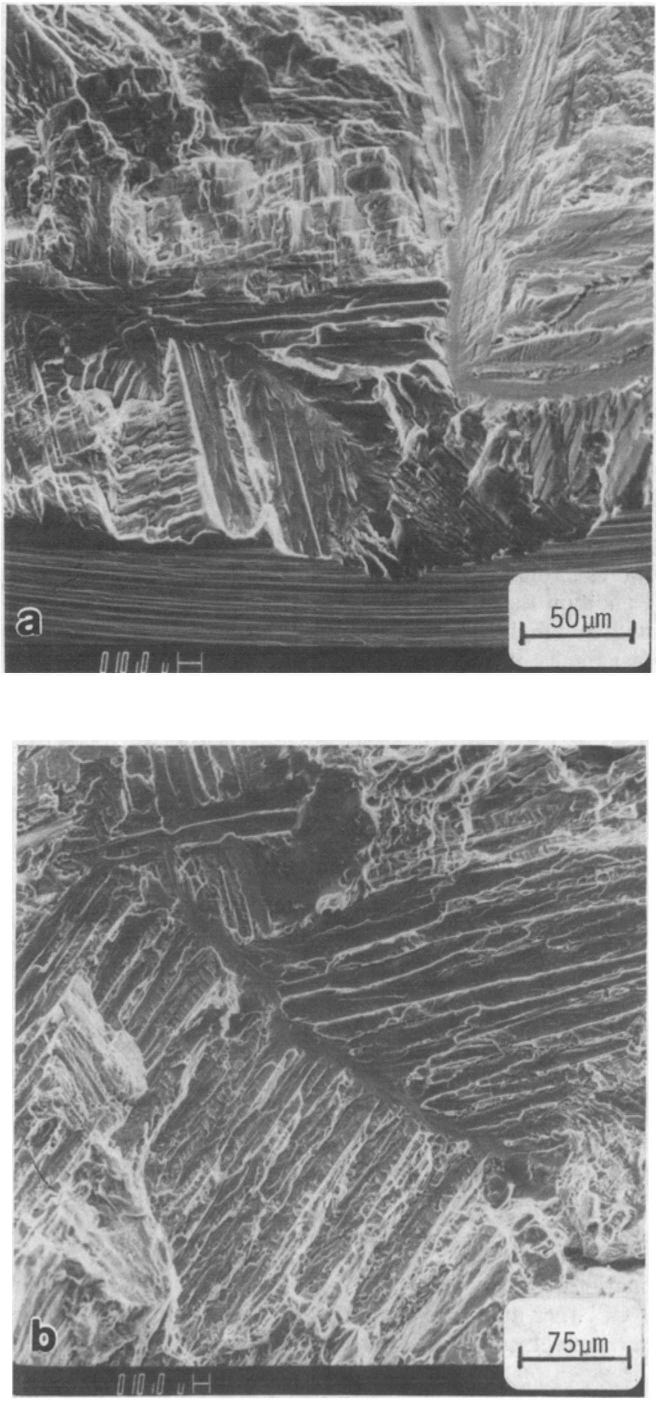


Fig. 8—(*a*) Multi-colony initiation facet and (*b*) multi-colony propagation facet.

size does not promote early fatigue crack initiation. Initial work has shown that this critical size could be as large as 50 microns.[13]

## IV. SUMMARY AND CONCLUSIONS

A wide range of microstructures was developed in HIP consolidated REP Ti-6Al-4V powder compacts by thermomechanical processing and was evaluated for low cycle fatigue (LCF) behavior.

1. These conditions demonstrated better LCF strength than previously tested PM material which had a higher contaminant level and also lower strength level.
2. Conditions with similar microstructures like Conditions 1 and 3 or Conditions 2 and 4 exhibited similar fatigue results.
3. In the five microstructural conditions tested, the fatigue strength increased with increasing tensile strength, decreasing primary alpha size, and decreasing alpha aspect ratio. As a result, Condition 4 (alpha + beta worked and solution treated) demonstrated the highest fatigue strength and the beta annealed material, Condition 5, had the lowest fatigue strength.
4. Fatigue failure initiation sites were not associated with contaminants or pores. In particular, no crack initiation at tungsten particles was seen in the present work.
5. Most alpha + beta worked and solution treated Condition 4 specimens showed fatigue initiations at subsurface locations. These locations were not associated with defects or lower fatigue life.
6. All conditions (except the beta-annealed Condition 5), demonstrated fatigue strength higher than reported in other work on PM material and were within the fatigue scatterband of mill annealed wrought alloy material with a typical tensile strength of 960 MPa.
7. Some porosity was present, which may have been thermally induced. However, this was not associated with crack initiation and did not appear to cause any detectable reduction in fatigue life.

## ACKNOWLEDGMENTS

The authors would like to express their appreciation to Mr. R. Vaughan of IMI, Mr. V. C. Petersen and Mr. C. F. Yolton of Crucible Research Center, and Mr. H. Holl of the Royal Aircraft Establishment for their contributions to this program. The assistance of Dr. I. Martorell in processing the compacts is greatly appreciated. In addition, the experimental assistance of Mr. S. W. Schwenker and Mr. N. G. Lovell, and helpful discussions with Mr. P. R. Smith are acknowledged. Parts of this work were done under USAF Contract F33615-79-C-5152 and UK MoD Contract A91A/354.

## REFERENCES

1. *Powder Metallurgy of Titanium Alloys*, F. H. Froes and John E. Smugeresky, eds., TMS-AIME Publications, Warrendale, PA, 1980, pp. 1-314.
2. F. H. Froes, D. Eylon, G. E. Eichelman, and H. M. Burte: *Journal of Metals*, 1980, vol. 32 (2), pp. 47-54.
3. C. A. Kelto, B. A. Kosmal, D. Eylon, and F. H. Froes: *Journal of Metals*, 1980, vol. 32 (8), pp. 17-25.
4. D. Eylon, M. Field, F. H. Froes, and G. E. Eichelman: *SAMPE Quarterly*, 1981, vol. 12, no. 3, pp. 19-25.
5. R. F. Vaughan, P. A. Blenkinsop, and P. H. Morton: *AGARD 1978*, Conference Proceedings No. 200, on Advanced Fabrication Techniques in Powder Metallurgy and Their Economic Implications, pp. 11-1 to 11-7.
6. R. E. Peebles and C. A. Kelto: Reference 1, pp. 47-58.
7. D. Eylon and F. H. Froes: ASTM STP 796 on *Titanium Alloys in Surgical Implants*, H. A. Luckey and F. Kubli, eds., ASTM Publications, Philadelphia, PA, 1983, pp. 43-58.
8. F. H. Froes and D. Eylon: *Progress in Powder Metallurgy*, 1981, vol. 37, pp. 279-88.

9. P. R. Smith, D. Eylon, S. W. Schwenker, and F. H. Froes: *Advanced Processing Methods for Titanium*, D. F. Hasson and C. H. Hamilton, eds., TMS-AIME Publications, Warrendale, PA, 1982, pp. 61-77.
10. F. H. Froes, D. Eylon, G. Wirth, K-J. Grundhoff, and W. Smarsly: *Metals Powder Reports*, MPR Publications, Shrewsbury, UK, 1983, vol. 38, no. 1, pp. 36-41.
11. P. R. Roberts and P. Loewenstein: Reference 1, pp. 21-36.
12. W. Betz and W. Track: "Living with Defects in PM Materials," Proceedings of *Powder Metallurgy Superalloys*, a Metal Powder Report Conference, Zurich, Switzerland, November 1980.
13. S. W. Schwenker, D. Eylon, and F. H. Froes: Proceedings of the 28th SAMPE National Symposium, Anaheim, CA, Society for the Advancement of Materials and Process Engineering, Azusa, CA, 1983, in press.
14. E. J. Dulis, V. K. Chandhok, F. H. Froes, and L. P. Clark: Proceedings of the 10th National SAMPE Technical Conference, *Materials Synergism*, published by Society for the Advancement of Materials and Process Engineering, Azusa, CA, 1978, vol. 10, pp. 316-29.
15. D. Eylon, M. E. Rosenblum, and S. Fujishiro: *Titanium '80, Science and Technology*, H. Kimura and O. Izumi, eds., TMS-AIME Publications, Warrendale, PA, 1980, pp. 1845-54.
16. D. Eylon and C. M. Pierce: *Metall. Trans. A*, 1976, vol. 7A, pp. 111-21.
17. D. Eylon, J. A. Hall, C. M. Pierce, and D. L. Ruckle: *Metall. Trans. A*, 1976, vol. 7A, pp. 1817-26.
18. I. Weiss: Wright State University, Dayton, OH, private communication, 1983.
19. D. Eylon and J. A. Hall: *Metall. Trans. A*, 1977, vol. 8A, pp. 981-90.
20. D. Eylon: *Journal of Materials Science*, 1979, vol. 14, pp. 1914-22.
21. N. G. Lovell and D. Eylon: Metcut-Materials Research Group, Wright-Patterson AFB, OH, unpublished work, 1981.
22. S. W. Schwenker, D. Eylon, and F. H. Froes: Wright-Patterson AFB, OH, unpublished work, 1983.
23. S. Fujishiro and D. Eylon: *Metall. Trans. A*, 1980, vol. 11A, pp. 1259-63.
24. C. L. Hoffman, D. Eylon, and A. J. McEvily: ASTM STP 770 on *Low Cycle Fatigue and Life Prediction*, C. Amzallag, B. N. Leis, and P. Rabbe, eds., ASTM Publications, Philadelphia, PA, 1982, pp. 5-23.
25. D. Eylon: *Metall. Trans. A*, 1979, vol. 10A, pp. 311-17.
26. D. L. Davidson and D. Eylon: *Metall. Trans. A*, 1980, vol. 11A, pp. 837-43.
27. D. Shechtman and D. Eylon: *Metall. Trans. A*, 1978, vol. 9A, pp. 1018-20.